Disentangling linkages between satellite derived forest structure and productivity essential biodiversity variables.

Evan R. Muise[a,*], Margaret E. Andrew[b], Nicholas C. Coops[a], Txomin Hermosilla[c], A. Cole Burton[a], Stephen S. Ban[d]

[a] *University of British Columbia, Forest Resources Management, 2424 Main Mall, Vancouver, BC, Canada, V6T 1Z4*
[b] *Murdoch University, Environmental and Conservation Sciences and Harry Butler Institute, Murdoch, WA, Australia, 6150*
[c] *Natural Resources Canada, Canada Forest Service (Pacific Forestry Centre), 506 Burnside Rd W, Victoria, BC, Canada, V8Z 1M5*
[d] *Ministry of Environment and Climate Change Strategy, BC Parks, 525 Superior Street, Victoria, BC, Canada, V8V 1T7*

Abstract

[insert abstract here - nicholas ignore the formatting on the authors for now, i can output to pdf and have it formatted nicely for submission]

Keywords: remote sensing, landsat, forest structure, forest productivity, dynamic habitat indices, essential biodiversity variables

1. Introduction

With biodiversity being in decline, and facing extinction rates above the background extinction rate (Thomas et al., 2004; Urban, 2015), as well as the homogenization of communities at various scales (McGill et al., 2015) it is integral to be able to monitor how biodiversity is changing across the globe. In response, the global biodiversity community is making efforts to assess and halt the degradation of biodiversity. The Group for Earth Observation Biodiversity Observation Network has developed the Essential Biodiversity Variables (EBVs, Pereira et al., 2013), designed as an analog to the Essential Climate Variables framework (Bojinski et al., 2014). EBVs are designed to be global in scope, relevant to biodiversity information, feasible to use, and complementary to one another (Skidmore et al., 2021). While it can be incredibly difficult, time consuming, and expensive to collect data on biodiversity across wide swaths of land and varying ecosystems, EBVs, which can be correlated to sampled biodiversity information, allow for the monitoring and asssessment of protected area effectiveness and ecosystem health at large spatial scales (Hansen et al., 2021). There are six EBV classes, each of which correspond to a different facet of biodiversity including species populations, species traits, community composition, ecosystem structure, ecosystem function, and genetic composition (Pereira et al., 2013).

*Corresponding author
Email addresses: evan.muise@student.ubc.ca (Evan R. Muise), M.Andrew@murdoch.edu.au (Margaret E. Andrew), nicholas.coops@ubc.ca (Nicholas C. Coops), txomin.hermosillagomez@NRCan-RNCan.gc.ca (Txomin Hermosilla), cole.burton@ubc.ca (A. Cole Burton), Stephen.Ban@gov.bc.ca (Stephen S. Ban)

Satellite remote sensing has proven to be capable of measuring five of the six EBV classes, the exception being genetic composition, which requires in-situ observation and sampling (Skidmore et al., 2021). Species populations - and in turn community composition - can be assessed with very-high-resolution imagery to identify tree species at the tree-crown scale, however it is difficult and computationally expensive to extend these analyses to broader extents (Fassnacht et al., 2016; Graves et al., 2016) while species traits such as vegetation phenology have been observed at the single-tree scale using, for example, PlanetScope imagery and drone-based measurements (Wu et al., 2021). However, the spatially limited and often *ad-hoc* data collection approaches associated with monitoring individuals is not conducive to the global or regional scales required for biodiversity trend assessment (Valdez et al., 2023).

The two landscape-level EBVs (ecosystem structure and function) are well suited to be examined at large spatial scales using coarser spatial measurements, such as those taken from satellites by the Moderate Resolution Imaging Spectroradiometer [MODIS; Zhang et al. (2003)], the Landsat imaging systems (Fisher et al., 2006), or Sentinel-2 (Helfenstein et al., 2022; Darvishzadeh et al., 2019) programs. These mid-resolution satellites can monitor processes at broader extents but the coarse spatial resolution removes the ability to relate these traits to individual organisms. As a result, satellite remote sensing data has been shown to be arguably the most effective at monitoring ecosystem based EBVs focused on structure and function. These EBVs classes can be monitored at regional to global extents through the use of optical imagery (Cohen and Goward, 2004), as well as active sensors such as lidar (light detection and ranging) and radar (Guo et al., 2017; Lefsky et al., 2002; Lang et al., 2021; Neuenschwander and Pitts, 2019; Coops et al., 2016).

1.1. EBV - Ecosystem Structure

Forest structural diversity has been linked to biodiversity at various scales (Guo et al., 2017; Bergen et al., 2009; Gao et al., 2014). Structural attributes range in complexity from simple (canopy cover; canopy height), to more complex (vertical and horizontal structural complexity) to modelled (aboveground biomass; basal area), all of which can be assessed using lidar data (Coops et al., 2021). A suite of these lidar-derived attributes have been used as local indicators of biodiversity, including simple metrics such as canopy cover and canopy height as well as derived metrics including vertical profiles, aboveground biomass (Lefsky et al., 1999; Guo et al., 2017; Coops et al., 2016). Other second order derived metrics such as canopy texture, height class distribution, edges, and patch metrics have also been used to examine habitat and biodiversity at landscape scales (Bergen et al., 2009). Advances in satellite remote sensing processing have allowed 3D forest structure data to be imputed across wide spatial scales (Matasci et al., 2018; Coops et al., 2021) using data fusion approaches involving collected lidar data and optical/radar data.

Increased forest structural complexity has been hypothesized to create additional niches, leading to increased species diversity (Bergen et al.,

2009), which has been frequently demonstrated using avian species diversity metrics (Macarthur and Macarthur, 1961). For example: Herniman et al. (2020) used spectral and lidar derived forest structure data to model avian habitat suitability; Clawges et al. (2008) found that lidar derived forest structural attributes are capable of identifying habitat types associated with avian species in pine/aspen forests; Goetz et al. (2007) used canopy structural diversity to predict bird species richness, finding that canopy vertical distribution was the strongest predictor of species richness. Forest structural metrics have also been used to study biodiversity in other clades as well (Davies and Asner, 2014; Nelson et al., 2005).

1.2. EBV - Ecosystem Function

With respect to ecosystem function, energy availability in an ecosystem has shown to be a predictor of species richness and abundances at various scales (Chase and Leibold, 2002; Radeloff et al., 2019; Coops et al., 2019; Razenkova et al.), and is measurable using satellite remote sensing via the use of various vegetation indices (Huete et al., 2002; Radeloff et al., 2019). Vegetation indices, which are indicative of photosynthetic activity, are commonly used as proxies of gross primary productivity (Huang et al., 2019). These vegetation indices have also been used to assess patterns in biodiversity at single time points (Bonn et al., 2004), and more recently, through yearly summaries of productivity (Berry et al., 2007; Radeloff et al., 2019). The relationship between energy availability and biodiversity occurs via various hypothesized mechanisms, such as the available energy hypothesis (Currie et al., 2004; Wright, 1983), the environmental stress hypothesis (Currie et al., 2004), and the environmental stability hypothesis (Williams and Middleton, 2008). These three hypotheses have in turn been linked to patterns of annual surface reflectance in remote sensing data (Berry et al., 2007; Radeloff et al., 2019).

Berry et al. (2007) first explored this idea by proposing the linkage of intra-annual summaries of MODIS derived GPP to dispersive bird species. This idea was further refined into the Dynamic Habitat Indices [DHIs; Coops et al. (2008)], which have now been shown to be well suited to assess the three aforementioned hypotheses at global scales (Radeloff et al., 2019). The cumulative DHI calculates the total amount of energy available in a given pixel over the course of a year. Cumulative DHI is strongly linked to the available energy hypothesis, which suggests that with greater available energy species richness will increase (Wright, 1983). The minimum DHI, which calculates the lowest productivity over the course of a year can be matched to the environmental stress hypothesis, which proposes that higher levels of minimum available energy will lead to higher species richness (Currie et al., 2004). Finally, the variation DHI, which calculates the coefficient of variance in a vegetation index through the course of a year, corresponds to the environmental stability hypothesis which states that lower energy variation throughout a year will lead to increased species richness (Williams and Middleton, 2008).

1.3. Biodiversity Monitoring with EBVs

Biodiversity monitoring programs often require a range of information in order to accurately assess changes in ecosystem integrity (Lindenmayer and Likens, 2010). Choosing datasets that are most closely related to the phenomenon of interest in a given application allows for direct connections to monitoring results and management actions (Pressey et al., 2021). With the advent of large-extent monitoring methods like satellite remote sensing, and a proliferation of potential EBVs datasets, it becomes important to assess the interrelationships between these datasets, and assess their complementary of the information to reduce duplication of efforts (Pereira et al., 2013; Skidmore et al., 2021). When strong relationships are present between EBV classes, it becomes possible to assess the ecological relationships between potential EBVs. On the other hand, when datasets do not appear related, they may be well suited to be used in monitoring programs together, as complementary EBVs.

Linkages between forest ecosystem structure and function have been examined within a remote sensing context for over 20 years (Huete et al., 2002, Knyazikhin et al. (1998); Myneni and Williams, 1994). While there is significant theoretical and empirical evidence for their relationship at single time points (within a single image) (Myneni and Williams, 1994), various relationship directions and shapes have been found between forest structure and function metrics (Ali, 2019). Hypothesized mechanisms such as niche complementary have shown that aboveground biomass increases with stand structure (Zhang et al., 2012), while asymmetric competition for light can reduce forest productivity with increased structural complexity (Bourdier et al., 2016). The relationship in particular between forest structural diversity metrics - which are now more accurately and comprehensively derived from lidar data - and temporal variation in functional metrics, specifically the metrics of ecosystem productivity via the DHI framework, have yet to be fully examined.

The overall goal of this paper is to assess patterns of forest ecosystem structure and function and their complementarity across a wide range of ecosystems encompassing significant environmental gradients. To do so, we synthesize data from moderate-scale remote-sensing derived metrics of forest structure, represented as both simple ALS-extracted metrics of canopy height, cover and vertical complexity, as well as modelled forest structure attributes including volume, and aboveground biomass, with a well-established remote sensing derived index on ecosystem function. Our first question is to examine how ecosystem structure and function complement one another across a large environmental gradient and then compare the simple and modelled representations of forest structure to different levels of ecosystem function. This question is important as it provides insights to the EBV community around complementarity of remote sensing metrics when describing the structure and function of ecosystems and proposes a method to examine potential overlap when generating remote sensing EBVs.

Our second question examines the independent and shared relationships of ecosystem structure

height and cover, with modelled forest structure, on ecosystem function. This provides insight into the choice of remote sensing attributes to use when developing EBVs within a single EBV class. Remote sensing datasets can comprise relatively unprocessed observations, in this case ALS measures of height and cover which are derived from the raw 3D point cloud vs modelled attributes, such as biomass and volume, which involve the use the statistical relationships with field data to transform the observations into more refined data products. Assessing which of these two (or combination of the two) approaches has stronger or weaker correlations with estimates of function provides insights into the choice of data used to build EBVs. Lastly, we examine how the primary and modelled structure attributes partition the variance of the DHIs within key biomes and forest types across a large environmental range, examining to what extent ecosystem and forest types impacts these relationships and thus providing insight into the applicability of these results globally.

2. Methods

2.1. Study Area

British Columbia is the westernmost province of Canada, and is home to a variety of terrestrial ecosystems. Approximately 64% of the province is forested, with large environmental and topographic gradients (Pojar et al., 1987; BC Ministry of Forests, 2003). The Biogeoclimatic Ecosystem Classification (BEC) system identifies 16 zones based on the dominant tree species and the ecosystems general climate. These zones can be further split into subzones, variants, and phases based on microclimate, precipitation, and topography (Pojar et al., 1987). To examine trends across the large environmental gradients, we group the BEC zones into five broad biomes, specifically, the south interior, northern, montane, alpine, and coastal groups similar to Hamann and Wang (2006).

{insert figure showing ecosystems of interest and grouped bec zones} need to remake figure showing ecosystems

{table showing elevations and climate ranges for each included bec zone}

2.2. Data

2.2.1. Forest Structure

We used a suite of forest structural attributes (canopy height, canopy cover, Lorey's height, overstory cover, basal area, aboveground biomass, gross stem volume, mean elevation, elevation standard deviation, and structural complexity [coefficient of variation in elevation returns]). This dataset was created at a 30 m spatial resolution according to Matasci et al. (2018). In brief, the method used a set of lidar collections and field plots across Canada, and imputed the remaining pixels using a random forest k-Nearest Neighbour approach on Landsat-derived surface reflectance and auxiliary data such as topography. Detailed information on the creation of this dataset can be found in Matasci et al. (2018).

2.2.2. Dynamic Habitat Indices

We use an established set of indices of annual productivity shown to be related to global biodvier-

stiy trends: the Dynamic Habitat Indices [Radeloff et al. (2019)]. The DHIs are a set of satellite remote sensing derived productivity variables that summarize the cumulative amount of available energy, the minimum available energy, and the variation in available energy throughout a given year [Berry et al. (2007); Radeloff et al. (2019)]. The DHIs have previously been produced at a global extent using MODIS imagery , and have been used to assess alpha (Radeloff et al., 2019) and beta[Andrew et al. (2012)] diversity, species abundances [Razenkova et al.], and construct novel ecoregionalizations (**?**Andrew et al., 2013) . Recent studies have began to examine how these indices can be constructed at a finer spatial resolution by using multi-annual Landsat imagery to generate a single synthetic year of monthly observations [Razenkova et al. (2022)].

The DHIs were calculated according to [Razenkova et al. (2022); RAZENKOVA LANDSAT DHI PAPER IN PRESS] for all of terrestrial British Columbia. In brief, Google Earth Engine (Gorelick et al., 2017) was used to obtain all valid Landsat pixels for a given study area, filtering out pixels containing shadows, slouds, and cloud shadows within each image (Zhu and Woodcock, 2012), then calculated the NDVI for each pixel in each image. They then calculated the median NDVI value for each month across the ten year time span (2011-2020) to generate a synthetic year of monthly data. The sum, minimum, and coefficient of variation across this synthetic year of NDVI values is then calculated. More detailed information can be found in {Razenkova In Press}.

2.3. Sampling

We conducted model-based sampling across the sixteen forest-dominated ecosystems found within British Columbia [BC figure reference, I have not made this figure yet]. Samples were randomly selected within each BEC zone, in undisturbed pixels. Each sampled pixel had to have a forested land cover class (coniferous, deciduous, mixed-wood, or wetland-treed), and be surrounded by the same land cover class. The land cover mask was generated by **?**, need to add to zotero using a best-available-pixel composite, and an inverse-distance weighted random forest approach across Canada. Additionally, each pixel had to have a coefficient of variation less than 0.5 in surrounding pixels in the two simplest forest structural attributes, canopy height and canopy cover. A maximum of 3000 samples were sampled in each BEC zone with a 1 km minimum sampling distance to reduce the effects of spatial autocorrelation. All variables were natural-log transformed and standardized. Variables containing zeros were natural-log plus one transformed. Sampling was conducted in R (R Core Team, 2022) version 4.2.2 using the **sgsR** package (Goodbody et al., 2023). Focal analyses for the land cover classes and coefficient of variation were calculated in Python version 3.9.

2.4. Analysis

2.4.1. Redundancy Analysis and Variation Partitioning

Redundancy analysis (RDA) and variation partitioning were used to relate the primary and modelled forest structure attributes to ecosystem function across a broad environment range. Redun-

dancy analysis functions similarly to a multiple linear regression, except it is capable of predicting multiple response variables. It accomplishes this by first running a multiple linear regression of each predictor variable on each response variable, then running a principle component analysis on the residuals from each multiple linear regression. This reduces the dimensionality of the output, and allows the relationship strength to be assessed by calculating the loadings of both predictor and response variables on the RDA axes. Partial redundancy analysis function similarly, except also considers co-variates (Legendre and Legendre, 2012). Redundancy analysis has widely been used in community ecology where environmental variables of interest are compared to species composition (Blanchet et al., 2014; Kleyer et al., 2012). While RDA is common in the ecological literature, this analysis represents one of the first times this technique has been applied to assess the complimentary of proposed EBVs. Following the RDA, we employ ANOVAs to determine which axes are significant, and calculate the proportion of variance attributable to each axis using the eigenvalues generated from the RDA. We calculate axis loadings for both predictor and response variables by calculating the correlation between the variables and the RDA axes. Axis loadings represent the relationship between a given variable and the RDA axis. We only consider and display significant axes. To visualize the RDA for both predictor and response variables, we display the results as path diagrams, with loadings from each predictor to the RDA axis to the response variables. The variance explained by each axis is also displayed in the RDA box Figure 1. All RDA calculations were done in R (R Core Team, 2022) version 4.2.2 using the **vegan** package (Oksanen et al., 2022).

Variation partitioning is an extension of partial RDA which can assess the overlap between the explanatory power of two datasets by utilizing multiple partial RDAs and exchanging which datasets are considered the predictor, and which is considered the co-variate (Legendre and Legendre, 2012). Variation partitioning is traditionally displayed using a Venn diagram, in which the percentage of variance explained by each dataset is in a circle, and the overlap between circles represents the overlap in variance explained. All variation partition analyses were done in R (R Core Team, 2022) version 4.2.2 using the **vegan** package (Oksanen et al., 2022).

RDA and variation partitioning analyses were conducted for all samples, as well as individually across each BEC zone and forest type. The results were aggregated to BEC zone groups see 2.1 for visualization.

All code associated with the processing and analysis is available at https://github.com/emuise/codestructProdSem.

3. Results

Figure 1 A shows the results from redundancy analysis of forest structural attributes on the dynamic habitat indices across the entire sampled dataset. While there are three RDA axes associated with the full dataset, the third axis explains 0.05% of the variance in the DHIs, and as such we do not show it. The first axis is strongly represents

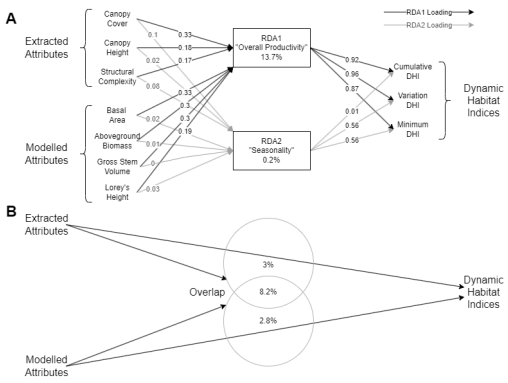

Figure 1: A) Axis loadings from redundancy analysis of primary and modelled forest structural attributes on the dynamic habitat indices. B) Results from variation partitioning of primary and modelled forest structural attributes on the DHIs. Both visualized analyses are across all collected samples. See supplementary information for results from each BEC zone and forest type.

all the DHIs (loadings > 0.85 for all DHIs), and has the strongest loadings from canopy cover, basal area, aboveground biomass, and gross stem volume. The other input attributes (canopy height, structural complexity, and Lorey's height) have smaller loadings. The second axis primarily represents the seasonality (Minimum and Variation DHI) of the DHIs, with a very small loading on the Cumulative DHI, and is primarily driven by canopy cover and complexity (Figure 1 A).

The results from the variation partitioning (Figure 1 B) show that the majority of the variance explained by the input datasets is shared across both primary and modelled attributes. 14% of the variation in the DHIs is explained by primary and modelled attributes, with 8.2% of this being from overlap between the datasets. The primary and modelled attributes explain 3 and 2.8% of the variation on their own, respectively (Figure 1 B).

A

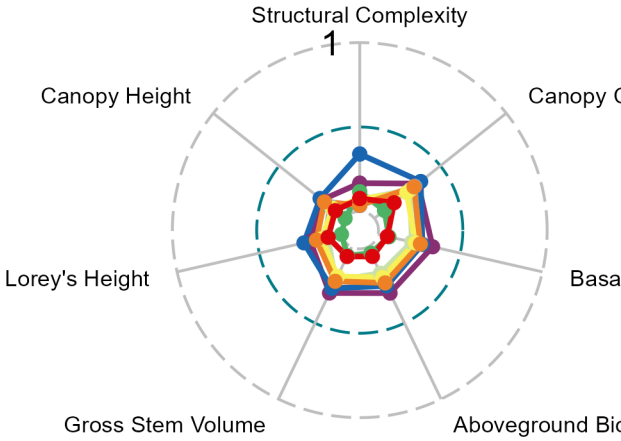

B

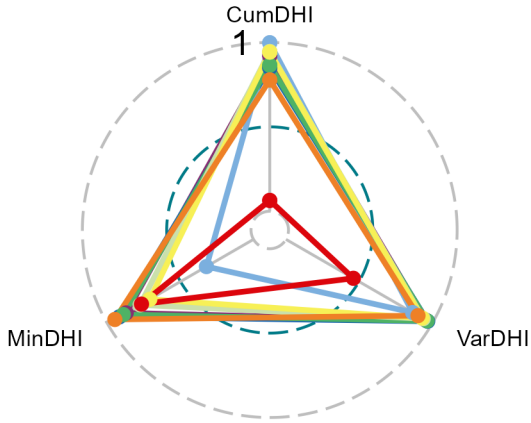

Figure 2: Radar plots of average loadings strength by group. A and B show input and response loadings, respectively. C) Boxplots of BEC zone, forest types, and all data loadings for predictor and response variables.

Figure 2 A and B show the axis loadings for predictor and response variables, respectively. Across the BEC zone groups, the loadings are generally similar in the predictor variables. Figure 2 C shows the individual BEC zone loadings. Canopy cover is generally the strongest predictor loading, and structural complexity is generally the weakest predictor loading. The exception is in deciduous forest types (mixed-wood and broadleaf), where structural complexity is the largest axis loading, alongside canopy cover (Figure 2 C). The second axis has smaller significant loadings.

For predictor variables, there are differences between the two axes. The first axis generally has large loadings across all DHIs, with the exception being alpine ecosystems, where the minimum DHI has lower loadings. The secondary RDA axis is primarily driven by variation in the minimum DHI, with medium loadings in the variation DHI, and small loadings in the cumulative DHI (Figure 2 B & C).

Figure 3 shows raincloud plots of the percentage of variation explained by predictor attributes in total, unique to modelled attributes, unique to primary attributes, and the overlap between primary and modelled attributes. Running the analysis by forest types generally results in higher amounts of variance explained, this is especially prevalent in deciduous forest types (mixed-wood and broadleaf). The overlap between modelled and primary attributes is generally higher than each dataset on their own (Figure 3). When the overlap explains a low amount variance, the information represented by the primary and modelled attributes are gener-

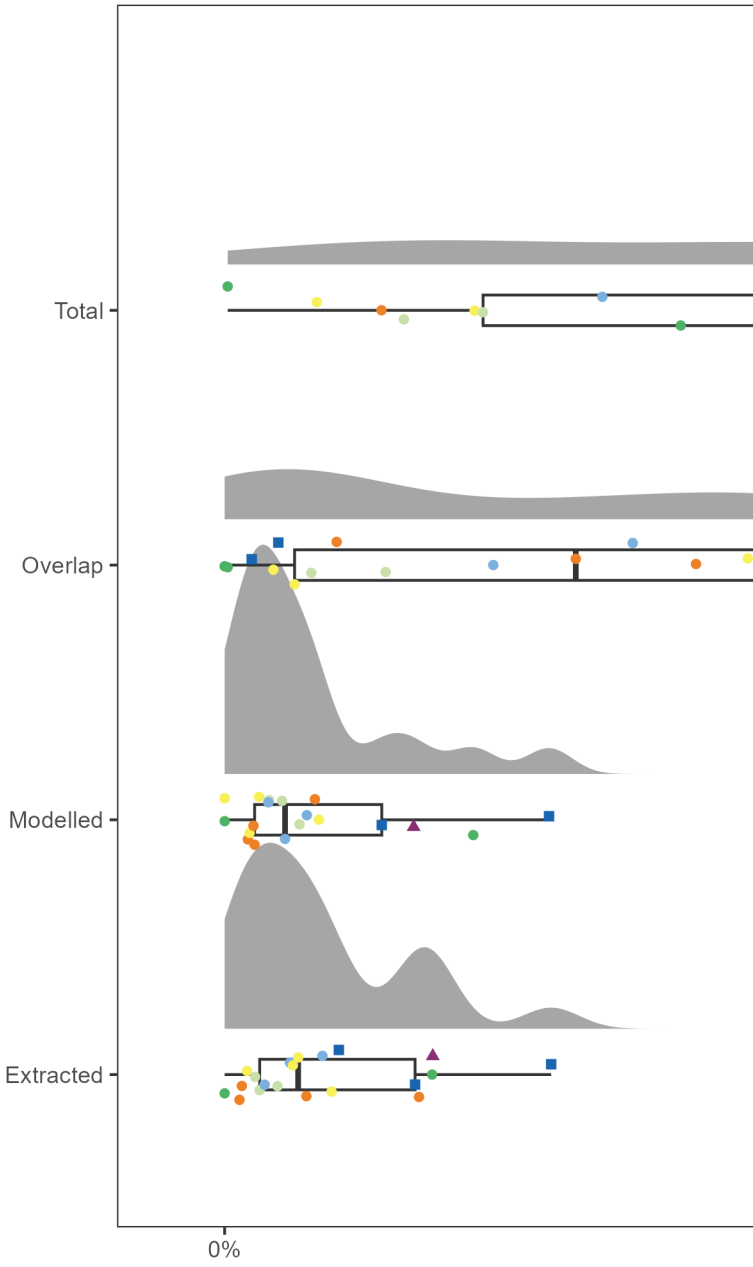

Figure 3: Raincloud plot of proportion of DHI variation explained by total, the overlap between primary and modelled structural attributes, and the overlap between primary and modelled attributes.

ally similar (i.e. in the all data analysis, 14% of the DHI's variance is explained by the strucutral data, with 8% being from the overlap, and 3% being from the primary and modelled attributes, respectively; Figure 1 A). Notably, the variation explained by the primary and modelled attributes is commonly presented through a single RDA axis, which generally corresponds to overall productivity through the year (Figure 2).

Figure 4 shows the proportion of variance explained as a proportion of a given BEC zone's forest that is coniferous. As the proportion of coniferous forest increases, so too does the amount of variance explained, while analyses ran on each forest type do not show a similar pattern (Figure 3).

Figure 5 shows false colour composites of primary (A & F), modelled (B & E), and DHI (C & F) loadings across the BEC zones of British Columbia. In the first RDA axis there is spatial variation in the primary attributes, with the centre of the province's axis being primarily driven by canopy cover (green), the coastal western hemlock zone (southwest coast) having a strong structural complexity loading, and the boreal in the northwest having the strongest loadings in canopy height (Figure 5 A). The modelled attributes generally show gray-scale colour, indicating that basal area, total biomass, and gross stem volume do not explain additional variation in the DHIs (Figure 5 B). Figure 5 C shows the loadings of the DHI, which are generally light tones, indicating high loadings across the province. Yellow shows a smaller minimum DHI loading, with higher loadings in the cumulative and variation DHIs.

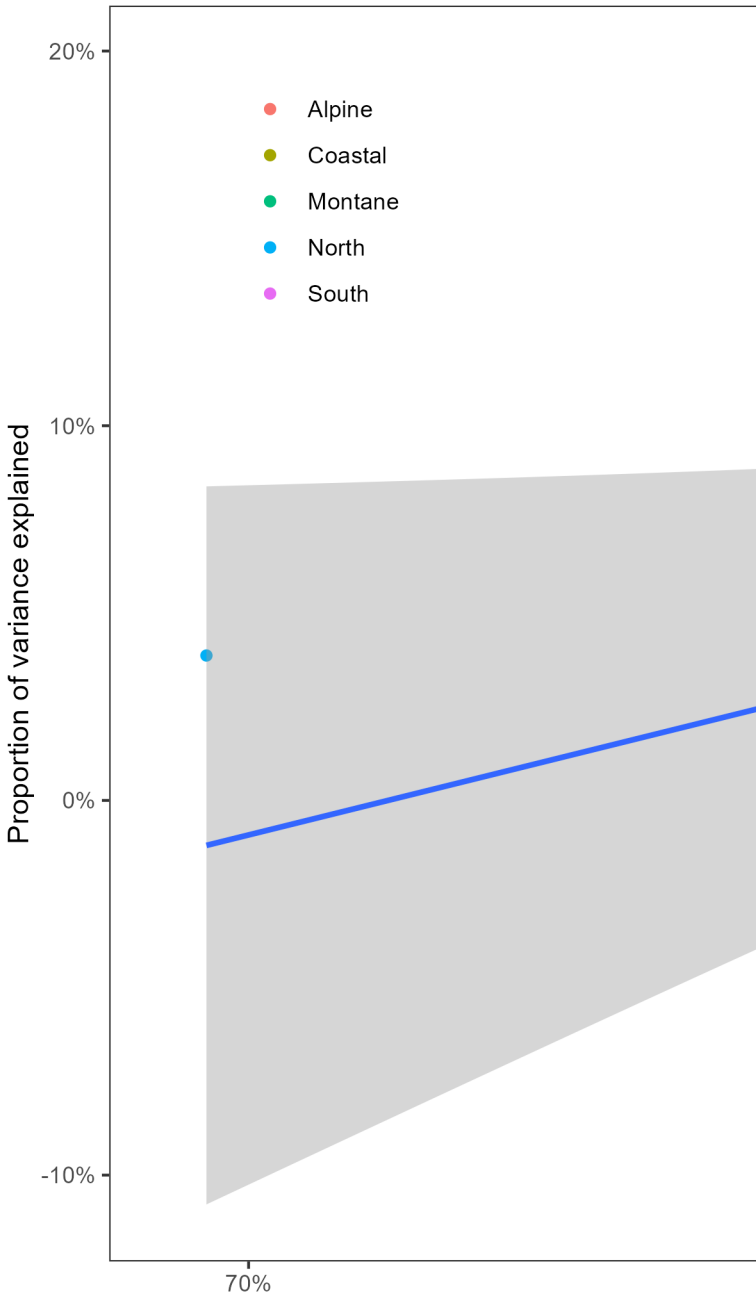

Figure 4: Proportion of variance explained by proportion of BEC zone's forest that are coniferous.

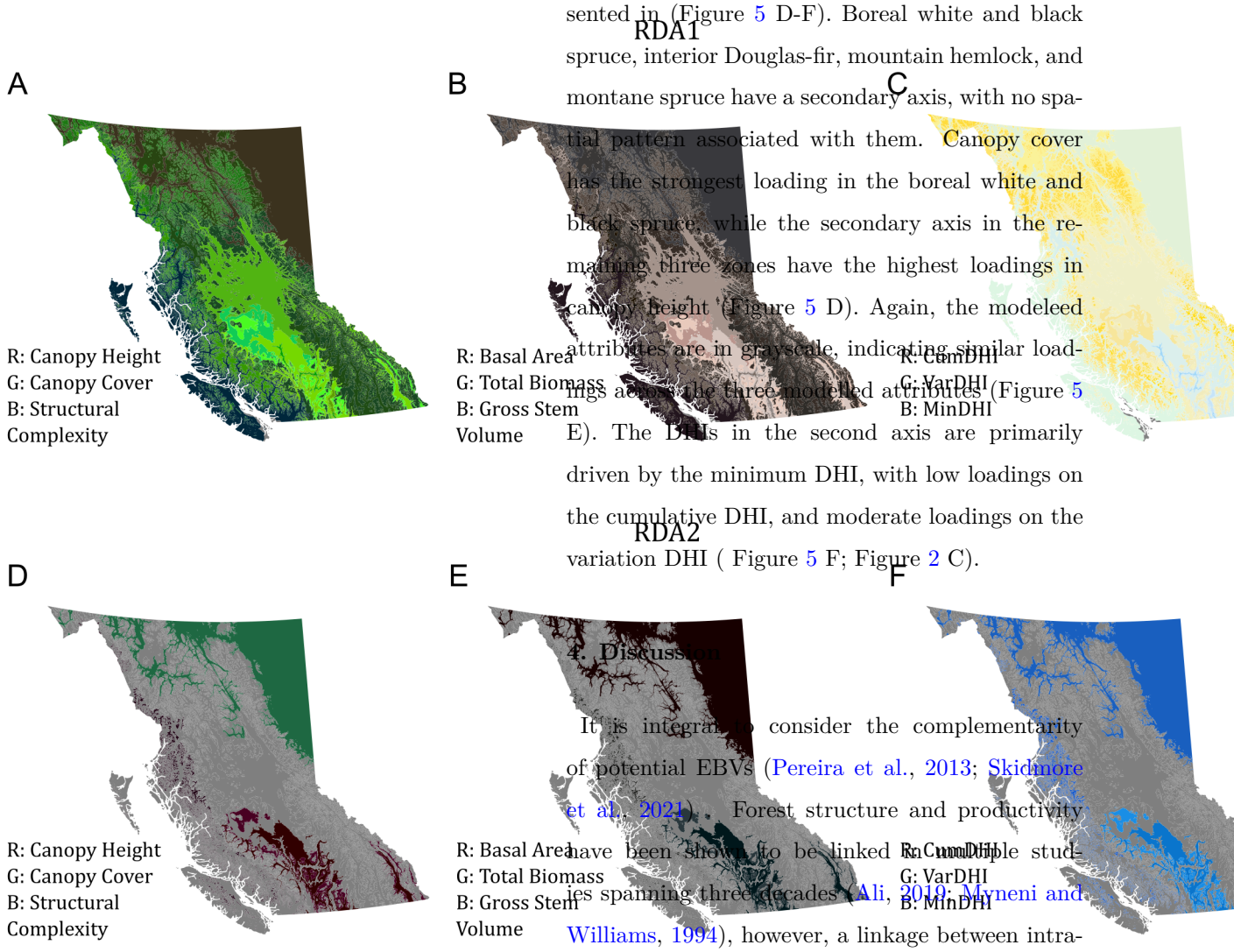

Figure 5: False colour maps of axis loadings for the first RDA axis (top) and second RDA axis (bottom). A and D show axis loadings for canopy height (r), canopy cover (g) and structural complexity (b). B and E show axis loadings for basal area(r), total biomass (g) and gross stem volume (b). C and F show axis loadings for the cumulative DHI (r), variation DHI (g) and minimum DHI (b).

Only four zones have a secondary RDA axis (Figure 2 C). These zones have been spatially represented in (Figure 5 D-F). Boreal white and black spruce, interior Douglas-fir, mountain hemlock, and montane spruce have a secondary axis, with no spatial pattern associated with them. Canopy cover has the strongest loading in the boreal white and black spruce, while the secondary axis in the remaining three zones have the highest loadings in canopy height (Figure 5 D). Again, the modeleed attributes are in grayscale, indicating similar loadings across the three modelled attributes (Figure 5 E). The DHIs in the second axis are primarily driven by the minimum DHI, with low loadings on the cumulative DHI, and moderate loadings on the variation DHI (Figure 5 F; Figure 2 C).

4. Discussion

It is integral to consider the complementarity of potential EBVs (Pereira et al., 2013; Skidmore et al., 2021). Forest structure and productivity have been shown to be linked in multiple studies spanning three decades (Ali, 2019; Myneni and Williams, 1994), however, a linkage between intra-annual production and forest structure has not been shown. In this study, we use statistical analyses from community ecology - namely redundancy analysis and variation partitioning - to assess the complementarity of forest structure and yearly productivity summaries. We find that the datasets do not strongly overlap, with forest structure explaining 14% of the variation in the dynamic habitat indices in samples taken across the entirety of British Columbia (Figure 1 B). This indicates that they

are suitable to be used in tandem with one another when used as ecosystem EBVs.

Across most of British Columbia's ecosystem, we identified a single RDA axis associated with the DHIs, encompassing the overall productivity (Figure 1 A). Within this first axis, the strongest loadings were canopy cover and the modelled attributes. When a second axis was significant, it consistently had strong loadings on the minimum and variation DHIs indicating a complex relationship within the DHIs in certain ecosystems. This secondary axis has smaller axis loadings associated with the primary and modelled attributes, with the strongest loadings being canopy cover and structural complexity across the entire dataset (Figure 1 A).

We also sought to explore whether modelled attributes (basal area, gross stem volume, aboveground biomass, and Lorey's height) add additional explanatory information when predicting the DHIs, as compared to primary forest structural attributes. We generally found that canopy cover had the largest axis loadings in the first RDA axis (Figure 2), which corresponds with canopy cover and LAI intercepting radiation from the sun influencing the amount of energy available in the environment (Knyazikhin et al., 1998). Modelled attributes such as basal area, aboveground biomass, and gross stem volume shared similar loading magnitudes across the range of studied ecosystems, indicating they do not add additional value when compared to one another (Figure 2 C; Figure 5 B). The loadings between the modelled attributes and canopy cover are often similar, and as such, we recommend utilizing the attributes derived directly from the point cloud in the case of ALS data, or selecting a single modelled attribute.

During the analysis we noticed a high amount of total variance explained in deciduous forests (mixed-wood and broadleaf) when compared to the other two forest types and most BEC zones. This could possibly be due to the loss of canopy cover during the winter being linked more closely to the DHIs, which are an annual summary of productivity, and not taken at a single time point, reducing the potential temporal mismatch between the two datasets. Further, the strongest loadings in these two forest types was vertical structural complexity, rather than canopy cover. This could indicate that in deciduous forests, additional leaf density at multiple layers is more important for productivity than canopy cover.

BEC zones dominated by coniferous forests tended to have higher amounts of variance explained by the structural attributes (Figure 4). This appears to be contrary to the observation that mixed-wood and broadleaf forests have much higher amounts of variation explained, and an analysis consisting solely of coniferous pixels has relatively low amounts of variance explained (Figure 3). This could be due to the large range in ecosystem variation across the province in coniferous forests. Running a similar analysis across each forest type and each BEC zone could increase the amount of explained variation, as the structural datasets would likely have less internal variation.

Finally, we explored the amount of variation explained by primary vs modelled attributes, as well

as their overlap (Figure 3). We generally found that the overlap between the primary and modelled attributes explained most of the variation, with some exceptions, indicating that using either set of forest structural attributes is suitable when monitoring biodiversity.

Recent advances in creating synthetic yearly observations have allowed the DHIs to be generated at a Landsat scale (30 m), rather than the previously used 250 m DHIs derived from MODIS [is the razenkova paper out yet???; Radeloff et al. (2019); Razenkova et al. (2022)]. This allows these datasets to be matched and analyzed with other datasets generated from the Landsat archive. This represents a significant advancement when assessing the utility of EBVs, as the 30 m scale is well suited to examine a range of ecological applications, including forest structure and productivity (Cohen and Goward, 2004).

In conclusion, we used redundancy analysis and variation partitioning to assess the complimentarity of two potential EBV datasets - forest structure and the DHIs. We also separated the forest structure datasets into primary and modelled attributes in order to assess the need to develop more complex structural attributes, or if base data derived directly from lidar datasets was suitable. We found that the structural attributes are not strongly related to the DHIs, indicating that they are suitable to be used together as ecosystem scale EBVs when monitoring forest environments. We also found that variation explained by the overlap between primary and modelled attributes was often higher than the variation explained by either individually.

Further research could assess the importance on intra-annual productivity vs the single time point of forest strucutre, which does not strongly change throughout the yaer (barring large disturbances).

References

Ali, A., 2019. Forest stand structure and functioning: Current knowledge and future challenges. Ecological Indicators 98, 665–677. URL: https://gateway.webofknowledge.com/gateway/Gateway.cgi?GWVersion=2&SrcAuth=DOISource&SrcApp=WOS&KeyAID=10.1016%2Fj.ecolind.2018.11.017&DestApp=DOI&SrcAppSID=8ErhQvgXXQBtHJO9AGH&SrcJTitle=ECOLOGICAL+INDICATORS&DestDOIRegistrantName=Elsevier, doi:10.1016/j.ecolind.2018.11.017. place: Amsterdam Publisher: Elsevier WOS:000464891100067.

Andrew, M.E., Nelson, T.A., Wulder, M.A., Hobart, G.W., Coops, N.C., Farmer, C.J.Q., 2013. Ecosystem classifications based on summer and winter conditions. Environmental Monitoring and Assessment 185, 3057–3079. doi:10.1007/s10661-012-2773-z. pMID: 22832845.

Andrew, M.E., Wulder, M.A., Coops, N.C., Baillargeon, G., 2012. Beta-diversity gradients of butterflies along productivity axes. Global Ecology and Biogeography 21, 352–364. URL: https://onlinelibrary.wiley.com/doi/abs/10.1111/j.1466-8238.2011.00676.x, doi:10.1111/j.1466-8238.2011.00676.x. _eprint: https://onlinelibrary.wiley.com/doi/pdf/10.1111/j.1466-8238.2011.00676.x.

BC Ministry of Forests, 2003. British Columbia's Forests and their Management. Technical Report. URL: https://www.for.gov.bc.ca/hfd/pubs/docs/mr/mr113/forests.htm.

Bergen, K.M., Goetz, S.J., Dubayah, R.O., Henebry, G.M., Hunsaker, C.T., Imhoff, M.L., Nelson, R.F., Parker, G.G., Radeloff, V.C., 2009. Remote sensing of vegetation 3-d structure for biodiversity and habitat: Review and implications for lidar and radar spaceborne missions. Journal of Geophysical Research-Biogeosciences 114, G00E06. URL: https://www.webofscience.com/api/gateway?GWVersion=2&SrcAuth=DOISource&SrcApp=WOS&KeyAID=10.1029%2F2008JG000883&DestApp=DOI&SrcAppSID=USW2EC0FB0f86g21rqa8mTRWHZ2vU&SrcJTitle=JOURNAL+OF+GEOPHYSICAL+RESEARCH-BIOGEOSCIENCES&DestDOIRegistrantName=American+Geophysical+Union, doi:10.1029/2008JG000883. place: Washington Publisher: Amer Geophysical Union WOS:000273047000001.

Berry, S., Mackey, B., Brown, T., 2007. Potential applications of remotely sensed vegetation greenness to habitat analysis and the conservation of dispersive fauna. Pacific Conservation Biology 13, 120–127. URL: https://www.proquest.com/docview/862947552/abstract/BE4B5C1D02174266PQ/1, doi:10.1071/PC070120. num Pages: 8 Place: Clayton, Australia Publisher: CSIRO.

Blanchet, F.G., Legendre, P., Bergeron, J.A.C., He, F., 2014. Consensus rda across dissimilarity coefficients for canonical ordination of community composition data. Ecological Monographs 84, 491–511. URL: https://onlinelibrary.wiley.com/doi/abs/10.1890/13-0648.1, doi:10.1890/13-0648.1. _eprint: https://onlinelibrary.wiley.com/doi/pdf/10.1890/13-0648.1.

Bojinski, S., Verstraete, M., Peterson, T.C., Richter, C., Simmons, A., Zemp, M., 2014. The concept of essential climate variables in support of climate research, applications, and policy. Bulletin of the American Meteorological Society 95, 1431–1443. URL: https://journals.ametsoc.org/view/journals/bams/95/9/bams-d-13-00047.1.xml, doi:10.1175/BAMS-D-13-00047.1.

Bonn, A., Storch, D., Gaston, K.J., 2004. Structure of the species–energy relationship. Proceedings of the Royal Society of London. Series B: Biological Sciences 271, 1685–1691. URL: https://royalsocietypublishing.org/doi/10.1098/rspb.2004.2745, doi:10.1098/rspb.2004.2745.

Bourdier, T., Cordonnier, T., Kunstler, G., Piedallu, C., Lagarrigues, G., Courbaud, B., 2016. Tree size inequality reduces forest productivity: An analysis combining inventory data for ten european species and a light competition model. PLOS ONE 11, e0151852. URL: https://journals.plos.org/plosone/article?id=10.1371/journal.pone.0151852, doi:10.1371/journal.pone.0151852. publisher: Public Library of Science.

Chase, J.M., Leibold, M.A., 2002. Spatial scale dictates the productivity–biodiversity relationship. Nature 416, 427–430. URL: https://www.nature.com/articles/416427a,

doi:10.1038/416427a. number: 6879 Publisher: Nature Publishing Group.

Clawges, R., Vierling, K., Vierling, L., Rowell, E., 2008. The use of airborne lidar to assess avian species diversity, density, and occurrence in a pine/aspen forest. Remote Sensing of Environment 112, 2064–2073. URL: https://linkinghub.elsevier.com/retrieve/pii/S0034425708000291, doi:10.1016/j.rse.2007.08.023. place: New York Publisher: Elsevier Science Inc WOS:000255370700012.

Cohen, W.B., Goward, S.N., 2004. Landsat's role in ecological applications of remote sensing. Bioscience 54, 535–545. doi:10.1641/0006-3568(2004)054[0535:LRIEAO]2.0.CO;2. place: Oxford Publisher: Oxford Univ Press WOS:000222020700011.

Coops, N.C., Bolton, D.K., Hobi, M.L., Radeloff, V.C., 2019. Untangling multiple species richness hypothesis globally using remote sensing habitat indices. ECOLOGICAL INDICATORS 107. doi:10.1016/j.ecolind.2019.105567. tex.article-number: 105567 tex.eissn: 1872-7034 tex.orcid-numbers: Radeloff, Volker C/0000-0001-9004-221X Hobi, Martina/0000-0003-3537-9738 tex.researcherid-numbers: Radeloff, Volker C/B-6124-2016 tex.unique-id: WOS:000490757500029.

Coops, N.C., Tompalski, P., Goodbody, T.R.H., Queinnec, M., Luther, J.E., Bolton, D.K., White, J.C., Wulder, M.A., van Lier, O.R., Hermosilla, T., 2021. Modelling lidar-derived estimates of forest attributes over space and time: A review of approaches and future trends. Remote Sensing of Environment 260, 112477. URL: https://www.sciencedirect.com/science/article/pii/S0034425721001954, doi:10.1016/j.rse.2021.112477.

Coops, N.C., Tompaski, P., Nijland, W., Rickbeil, G.J., Nielsen, S.E., Bater, C.W., Stadt, J.J., 2016. A forest structure habitat index based on airborne laser scanning data. Ecological Indicators 67, 346–357. URL: https://linkinghub.elsevier.com/retrieve/pii/S1470160X16300784, doi:10.1016/j.ecolind.2016.02.057.

Coops, N.C., Wulder, M.A., Duro, D.C., Han, T., Berry, S., 2008. The development of a canadian dynamic habitat index using multi-temporal satellite estimates of canopy light absorbance. ECOLOGICAL INDICATORS 8, 754–766. doi:10.1016/j.ecolind.2008.01.007. tex.eissn: 1872-7034 tex.orcid-numbers: Coops, Nicholas/0000-0002-0151-9037 Coops, Nicholas/0000-0002-0151-9037 Wulder, Michael A/0000-0002-6942-1896 Duro, Dennis/0000-0003-4314-6635 tex.researcherid-numbers: Coops, Nicholas/J-1543-2012 Coops, Nicholas/L-3652-2019 Wulder, Michael A/J-5597-2016 Duro, Dennis/B-2423-2008 tex.unique-id: WOS:000255625200033.

Currie, D.J., Mittelbach, G.G., Cornell, H.V., Field, R., Guégan, J.F., Hawkins, B.A., Kaufman, D.M., Kerr, J.T., Oberdorff, T., O'Brien, E., Turner, J.R.G., 2004. Predictions and tests of climate-based hypotheses of broad-scale variation in taxonomic richness. Ecology Letters 7, 1121–1134. URL: https://onlinelibrary.wiley.com/doi/abs/10.1111/j.1461-0248.2004.00671.x, doi:10.1111/j.1461-0248.2004.00671.x. _eprint: https://onlinelibrary.wiley.com/doi/pdf/10.1111/j.1461-0248.2004.00671.x.

Darvishzadeh, R., Skidmore, A., Abdullah, H., Cherenet, E., Ali, A., Wang, T., Nieuwenhuis, W., Heurich, M., Vrieling, A., O'Connor, B., Paganini, M., 2019. Mapping leaf chlorophyll content from sentinel-2 and rapideye data in spruce stands using the invertible forest reflectance model. International Journal of Applied Earth Observation and Geoinformation 79, 58–70. URL: https://linkinghub.elsevier.com/retrieve/pii/S0303243419300984, doi:10.1016/j.jag.2019.03.003. place: Amsterdam Publisher: Elsevier WOS:000466820700006.

Davies, A.B., Asner, G.P., 2014. Advances in animal ecology from 3d-lidar ecosystem mapping. Trends in Ecology & Evolution 29, 681–691. URL: https://www.webofscience.com/api/gateway?GWVersion=2&SrcAuth=DOISource&SrcApp=WOS&KeyAID=10.1016%2Fj.tree.2014.10.005&DestApp=DOI&SrcAppSID=USW2EC0FB0f86g21rqa8mTRWHZ2vU&SrcJTitle=TRENDS+IN+ECOLOGY+%26+EVOLUTION&DestDOIRegistrantName=Elsevier, doi:10.1016/j.tree.2014.10.005.

Fassnacht, F.E., Latifi, H., Sterenczak, K., Modzelewska, A., Lefsky, M., Waser, L.T., Straub, C., Ghosh, A., 2016. Review of studies on tree species classification from remotely sensed data. Remote Sensing of Environment 186, 64–87. URL: https://linkinghub.elsevier.com/retrieve/pii/

S0034425716303169, doi:10.1016/j.rse.2016.08.013. place: New York Publisher: Elsevier Science Inc WOS:000396382500006.

Fisher, J.I., Mustard, J.F., Vadeboncoeur, M.A., 2006. Green leaf phenology at landsat resolution: Scaling from the field to the satellite. Remote Sensing of Environment 100, 265–279. URL: https://linkinghub.elsevier.com/retrieve/pii/S0034425705003597, doi:10.1016/j.rse.2005.10.022. place: New York Publisher: Elsevier Science Inc WOS:000235115500011.

Gao, T., Hedblom, M., Emilsson, T., Nielsen, A.B., 2014. The role of forest stand structure as biodiversity indicator. Forest Ecology and Management 330, 82–93. URL: https://www.sciencedirect.com/science/article/pii/S0378112714004241, doi:10.1016/j.foreco.2014.07.007.

Goetz, S., Steinberg, D., Dubayah, R., Blair, B., 2007. Laser remote sensing of canopy habitat heterogeneity as a predictor of bird species richness in an eastern temperate forest, usa. Remote Sensing of Environment 108, 254–263. doi:10.1016/j.rse.2006.11.016.

Goodbody, T.R., Coops, N.C., Queinnec, M., 2023. sgsR: Structurally Guided Sampling. URL: https://CRAN.R-project.org/package=sgsR. r package version 1.4.0.

Gorelick, N., Hancher, M., Dixon, M., Ilyushchenko, S., Thau, D., Moore, R., 2017. Google earth engine: Planetary-scale geospatial analysis for everyone. Remote Sensing of Environment 202, 18–27. URL: https://www.sciencedirect.com/science/article/pii/S0034425717302900, doi:10.1016/j.rse.2017.06.031.

Graves, S.J., Asner, G.P., Martin, R.E., Anderson, C.B., Colgan, M.S., Kalantari, L., Bohlman, S.A., 2016. Tree species abundance predictions in a tropical agricultural landscape with a supervised classification model and imbalanced data. Remote Sensing 8, 161. URL: https://www.mdpi.com/2072-4292/8/2/161, doi:10.3390/rs8020161. number: 2 Publisher: Multidisciplinary Digital Publishing Institute.

Guo, X., Coops, N.C., Tompalski, P., Nielsen, S.E., Bater, C.W., John Stadt, J., 2017. Regional mapping of vegetation structure for biodiversity monitoring using airborne lidar data. Ecological Informatics 38, 50–61. URL: https://www.sciencedirect.com/science/article/pii/S1574954116300905, doi:10.1016/j.ecoinf.2017.01.005.

Hamann, A., Wang, T., 2006. Potential effects of climate change on ecosystem and tree species distribution in british columbia. Ecology 87, 2773–2786. URL: https://www.jstor.org/stable/20069297. publisher: Ecological Society of America.

Hansen, A.J., Noble, B.P., Veneros, J., East, A., Goetz, S.J., Supples, C., Watson, J.E.M., Jantz, P.A., Pillay, R., Jetz, W., Ferrier, S., Grantham, H.S., Evans, T.D., Ervin, J., Venter, O., Virnig, A.L.S., 2021. Toward monitoring forest ecosystem integrity within the post-2020 global biodiversity framework. Conservation Letters 14, e12822. URL: https://onlinelibrary.wiley.com/doi/abs/10.1111/conl.12822, doi:10.1111/conl.12822. _eprint: https://onlinelibrary.wiley.com/doi/pdf/10.1111/conl.12822.

Helfenstein, I.S., Schneider, F.D., Schaepman, M.E., Morsdorf, F., 2022. Assessing biodiversity from space: Impact of spatial and spectral resolution on trait-based functional diversity. Remote Sensing of Environment 275, 113024. URL: https://www.sciencedirect.com/science/article/pii/S0034425722001389, doi:10.1016/j.rse.2022.113024.

Herniman, S., Coops, N.C., Martin, K., Thomas, P., Luther, J.E., van Lier, O.R., 2020. Modelling avian habitat suitability in boreal forest using structural and spectral remote sensing data. Remote Sensing Applications: Society and Environment 19, 100344. URL: https://www.sciencedirect.com/science/article/pii/S2352938520300318, doi:10.1016/j.rsase.2020.100344.

Huang, X., Xiao, J., Ma, M., 2019. Evaluating the performance of satellite-derived vegetation indices for estimating gross primary productivity using fluxnet observations across the globe. Remote Sensing 11, 1823. URL: https://www.mdpi.com/2072-4292/11/15/1823, doi:10.3390/rs11151823. number: 15 Publisher: Multidisciplinary Digital Publishing Institute.

Huete, A., Didan, K., Miura, T., Rodriguez, E.P., Gao, X., Ferreira, L.G., 2002. Overview of the radiometric and biophysical performance of the modis vegetation indices. Remote Sensing of Environment 83, 195–213. URL: https://gateway.webofknowledge.com/gateway/Gateway.

cgi?GWVersion=2&SrcAuth=DOISource&SrcApp=WOS&KeyAID=10.1016%2FS0034-4257%2802%2900096-2&DestApp=DOI&SrcAppSID=6ABQuYtmtvvjzqEmPms&SrcJTitle=REMOTE+SENSING+OF+ENVIRONMENT&DestDOIRegistrantName=Elsevier, doi:10.1016/S0034-4257(02)00096-2. place: New York Publisher: Elsevier Science Inc WOS:000179160200014.

Kleyer, M., Dray, S., Bello, F., Lepš, J., Pakeman, R.J., Strauss, B., Thuiller, W., Lavorel, S., 2012. Assessing species and community functional responses to environmental gradients: which multivariate methods? Journal of Vegetation Science 23, 805–821. URL: https://onlinelibrary.wiley.com/doi/abs/10.1111/j.1654-1103.2012.01402.x, doi:10.1111/j.1654-1103.2012.01402.x. _eprint: https://onlinelibrary.wiley.com/doi/pdf/10.1111/j.1654-1103.2012.01402.x.

Knyazikhin, Y., Martonchik, J.V., Myneni, R.B., Diner, D.J., Running, S.W., 1998. Synergistic algorithm for estimating vegetation canopy leaf area index and fraction of absorbed photosynthetically active radiation from modis and misr data. Journal of Geophysical Research: Atmospheres 103, 32257–32275. URL: https://onlinelibrary.wiley.com/doi/abs/10.1029/98JD02462, doi:10.1029/98JD02462. _eprint: https://onlinelibrary.wiley.com/doi/pdf/10.1029/98JD02462.

Lang, N., Kalischek, N., Armston, J., Schindler, K., Dubayah, R., Wegner, J.D., 2021. Global canopy height estimation with gedi lidar waveforms and bayesian deep learning. arXiv:2103.03975 [physics] URL: http://arxiv.org/abs/2103.03975. arXiv: 2103.03975.

Lefsky, M.A., Cohen, W.B., Acker, S.A., Parker, G.G., Spies, T.A., Harding, D., 1999. Lidar remote sensing of the canopy structure and biophysical properties of douglas-fir western hemlock forests. Remote Sensing of Environment 70, 339–361. URL: https://gateway.webofknowledge.com/gateway/Gateway.cgi?GWVersion=2&SrcAuth=DOISource&SrcApp=WOS&KeyAID=10.1016%2FS0034-4257%2899%2900052-8&DestApp=DOI&SrcAppSID=USW2EC0C5Bes58CNu2bH9fPMaswk7&SrcJTitle=REMOTE+SENSING+OF+ENVIRONMENT&DestDOIRegistrantName=Elsevier, doi:10.1016/S0034-4257(99)00052-8. place: New York Publisher: Elsevier Science Inc WOS:000084296300009.

Lefsky, M.A., Cohen, W.B., Parker, G.G., Harding, D.J., 2002. Lidar remote sensing for ecosystem studies. Bioscience 52, 19–30. URL: https://academic.oup.com/bioscience/article/52/1/19/291259, doi:10.1641/0006-3568(2002)052[0019:LRSFES]2.0.CO;2. place: Oxford Publisher: Oxford Univ Press WOS:000173456700009.

Legendre, P., Legendre, L., 2012. Numerical Ecology. Elsevier.

Lindenmayer, D.B., Likens, G.E., 2010. The science and application of ecological monitoring. Biological Conservation 143, 1317–1328. URL: https://linkinghub.elsevier.com/retrieve/pii/S0006320710000522, doi:10.1016/j.biocon.2010.02.013.

Macarthur, R., Macarthur, J., 1961. On bird species-diversity. Ecology 42, 594–598. URL: https://www.webofscience.com/api/gateway?GWVersion=2&SrcAuth=DOISource&SrcApp=WOS&KeyAID=10.2307%2F1932254&DestApp=DOI&SrcAppSID=USW2EC0FB0f86g21rqa8mTRWHZ2vU&SrcJTitle=ECOLOGY&DestDOIRegistrantName=JSTOR, doi:10.2307/1932254.

Matasci, G., Hermosilla, T., Wulder, M.A., White, J.C., Coops, N.C., Hobart, G.W., Bolton, D.K., Tompalski, P., Bater, C.W., 2018. Three decades of forest structural dynamics over canada's forested ecosystems using landsat time-series and lidar plots. Remote Sensing of Environment 216, 697–714. URL: https://linkinghub.elsevier.com/retrieve/pii/S0034425718303572, doi:10.1016/j.rse.2018.07.024.

McGill, B.J., Dornelas, M., Gotelli, N.J., Magurran, A.E., 2015. Fifteen forms of biodiversity trend in the anthropocene. Trends in Ecology & Evolution 30, 104–113. URL: https://www.sciencedirect.com/science/article/pii/S0169534714002456, doi:10.1016/j.tree.2014.11.006.

Myneni, R.B., Williams, D.L., 1994. On the relationship between fapar and ndvi. Remote Sensing of Environment 49, 200–211. URL: https://www.sciencedirect.com/science/article/pii/0034425794900167, doi:10.1016/0034-4257(94)90016-7.

Nelson, R., Keller, C., Ratnaswamy, M., 2005. Locating and estimating the extent of delmarva fox squirrel habitat using an airborne lidar profiler. Remote Sensing of Environment 96, 292–301. URL: https://www.webofscience.com/api/gateway?GWVersion=2&SrcAuth=DOISource&SrcApp=WOS&KeyAID=10.1016%2Fj.rse.2005.02.012&DestApp=DOI&SrcAppSID=USW2EC0FB0f86g21rqa8mTRWHZ2vU&SrcJTitle=REMOTE+SENSING+OF+ENVIRONMENT&DestDOIRegistrantName=Elsevier, doi:10.1016/j.rse.2005.02.012.

Neuenschwander, A., Pitts, K., 2019. The atl08 land and vegetation product for the icesat-2 mission. Remote Sensing of Environment 221, 247–259. URL: https://linkinghub.elsevier.com/retrieve/pii/S0034425718305066, doi:10.1016/j.rse.2018.11.005.

Oksanen, J., Simpson, G.L., Blanchet, F.G., Kindt, R., Legendre, P., Minchin, P.R., O'Hara, R., Solymos, P., Stevens, M.H.H., Szoecs, E., Wagner, H., Barbour, M., Bedward, M., Bolker, B., Borcard, D., Carvalho, G., Chirico, M., De Caceres, M., Durand, S., Evangelista, H.B.A., FitzJohn, R., Friendly, M., Furneaux, B., Hannigan, G., Hill, M.O., Lahti, L., McGlinn, D., Ouellette, M.H., Ribeiro Cunha, E., Smith, T., Stier, A., Ter Braak, C.J., Weedon, J., 2022. vegan: Community Ecology Package. URL: https://github.com/vegandevs/vegan. r package version 2.6-4.

Pereira, H.M., Ferrier, S., Walters, M., Geller, G.N., Jongman, R.H.G., Scholes, R.J., Bruford, M.W., Brummitt, N., Butchart, S.H.M., Cardoso, A.C., Coops, N.C., Dulloo, E., Faith, D.P., Freyhof, J., Gregory, R.D., Heip, C., Hoft, R., Hurtt, G., Jetz, W., Karp, D.S., McGeoch, M.A., Obura, D., Onoda, Y., Pettorelli, N., Reyers, B., Sayre, R., Scharlemann, J.P.W., Stuart, S.N., Turak, E., Walpole, M., Wegmann, M., 2013. Essential biodiversity variables. Science 339, 277–278. URL: https://www.sciencemag.org/lookup/doi/10.1126/science.1229931, doi:10.1126/science.1229931.

Pojar, J., Klinka, K., Meidinger, D., 1987. Biogeoclimatic ecosystem classification in british columbia. Forest Ecology and Management 22, 119–154. URL: https://linkinghub.elsevier.com/retrieve/pii/0378112787901009, doi:10.1016/0378-1127(87)90100-9.

Pressey, R.L., Visconti, P., McKinnon, M.C., Gurney, G.G., Barnes, M.D., Glew, L., Maron, M., 2021. The mismeasure of conservation. Trends in Ecology & Evolution 36, 808–821. URL: https://www.sciencedirect.com/science/article/pii/S0169534721001816, doi:10.1016/j.tree.2021.06.008.

R Core Team, 2022. R: A Language and Environment for Statistical Computing. R Foundation for Statistical Computing. Vienna, Austria. URL: https://www.R-project.org/.

Radeloff, V.C., Dubinin, M., Coops, N.C., Allen, A.M., Brooks, T.M., Clayton, M.K., Costa, G.C., Graham, C.H., Helmers, D.P., Ives, A.R., Kolesov, D., Pidgeon, A.M., Rapacciuolo, G., Razenkova, E., Suttidate, N., Young, B.E., Zhu, L., Hobi, M.L., 2019. The dynamic habitat indices (dhis) from modis and global biodiversity. Remote Sensing of Environment 222, 204–214. URL: https://www.sciencedirect.com/science/article/pii/S0034425718305625, doi:10.1016/j.rse.2018.12.009.

Razenkova, E., Dubinin, M., Pidgeon, A.M., Hobi, M.L., Zhu, L., Bragina, E.V., Allen, A.M., Clayton, M.K., Baskin, L.M., Coops, N.C., Radeloff, V.C., . Abundance patterns of mammals across russia explained by remotely sensed vegetation productivity and snow indices .

Razenkova, E., Farwell, L.S., Elsen, P., Carroll, K.A., Pidgeon, A.M., Radeloff, V., 2022. Explaining bird richness with the dynamic habitat indices across the conterminous us 2022, B15A–05. URL: https://ui.adsabs.harvard.edu/abs/2022AGUFM.B15A..05R. conference Name: AGU Fall Meeting Abstracts ADS Bibcode: 2022AGUFM.B15A..05R.

Skidmore, A.K., Coops, N.C., Neinavaz, E., Ali, A., Schaepman, M.E., Paganini, M., Kissling, W.D., Vihervaara, P., Darvishzadeh, R., Feilhauer, H., Fernandez, M., Fernández, N., Gorelick, N., Geijzendorffer, I., Heiden, U., Heurich, M., Hobern, D., Holzwarth, S., Muller-Karger, F.E., Van De Kerchove, R., Lausch, A., Leitão, P.J., Lock, M.C., Mücher, C.A., O'Connor, B., Rocchini, D., Turner, W., Vis, J.K., Wang, T., Wegmann, M., Wingate, V., 2021. Priority list of biodiversity metrics to observe from space. Nature Ecology & Evolution URL: http://www.nature.com/articles/s41559-021-01451-x, doi:10.

1038/s41559-021-01451-x.

Thomas, C.D., Cameron, A., Green, R.E., Bakkenes, M., Beaumont, L.J., Collingham, Y.C., Erasmus, B.F.N., de Siqueira, M.F., Grainger, A., Hannah, L., Hughes, L., Huntley, B., van Jaarsveld, A.S., Midgley, G.F., Miles, L., Ortega-Huerta, M.A., Peterson, A.T., Phillips, O.L., Williams, S.E., 2004. Extinction risk from climate change. Nature 427, 5.

Urban, M.C., 2015. Accelerating extinction risk from climate change. Science 348, 571–573. URL: https://www.science.org/doi/10.1126/science.aaa4984, doi:10.1126/science.aaa4984.

Valdez, J.W., Callaghan, C.T., Junker, J., Purvis, A., Hill, S.L.L., Pereira, H.M., 2023. The undetectability of global biodiversity trends using local species richness. Ecography 2023, e06604. URL: https://onlinelibrary.wiley.com/doi/abs/10.1111/ecog.06604, doi:10.1111/ecog.06604. _eprint: https://onlinelibrary.wiley.com/doi/pdf/10.1111/ecog.06604.

Williams, S.E., Middleton, J., 2008. Climatic seasonality, resource bottlenecks, and abundance of rainforest birds: implications for global climate change. Diversity and Distributions 14, 69–77. URL: https://onlinelibrary.wiley.com/doi/abs/10.1111/j.1472-4642.2007.00418.x, doi:10.1111/j.1472-4642.2007.00418.x. _eprint: https://onlinelibrary.wiley.com/doi/pdf/10.1111/j.1472-4642.2007.00418.x.

Wright, D.H., 1983. Species-energy theory: An extension of species-area theory. Oikos 41, 496–506. URL: https://www.jstor.org/stable/3544109, doi:10.2307/3544109. publisher: [Nordic Society Oikos, Wiley].

Wu, S., Wang, J., Yan, Z., Song, G., Chen, Y., Ma, Q., Deng, M., Wu, Y., Zhao, Y., Guo, Z., Yuan, Z., Dai, G., Xu, X., Yang, X., Su, Y., Liu, L., Wu, J., 2021. Monitoring tree-crown scale autumn leaf phenology in a temperate forest with an integration of planetscope and drone remote sensing observations. ISPRS Journal of Photogrammetry and Remote Sensing 171, 36–48. URL: https://www.sciencedirect.com/science/article/pii/S0924271620302975, doi:10.1016/j.isprsjprs.2020.10.017.

Zhang, X.Y., Friedl, M.A., Schaaf, C.B., Strahler, A.H., Hodges, J.C.F., Gao, F., Reed, B.C., Huete, A., 2003. Monitoring vegetation phenology using modis. Remote Sensing of Environment 84, 471–475. doi:10.1016/S0034-4257(02)00135-9. place: New York Publisher: Elsevier Science Inc WOS:000181591800011.

Zhang, Y., Chen, H.Y.H., Reich, P.B., 2012. Forest productivity increases with evenness, species richness and trait variation: a global meta-analysis. Journal of Ecology 100, 742–749. URL: https://onlinelibrary.wiley.com/doi/abs/10.1111/j.1365-2745.2011.01944.x, doi:10.1111/j.1365-2745.2011.01944.x. _eprint: https://onlinelibrary.wiley.com/doi/pdf/10.1111/j.1365-2745.2011.01944.x.

Zhu, Z., Woodcock, C.E., 2012. Object-based cloud and cloud shadow detection in landsat imagery. Remote Sensing of Environment 118, 83–94. URL: https://www.sciencedirect.com/science/article/pii/S0034425711003853, doi:10.1016/j.rse.2011.10.028.